Article

Received: 25.09.2023
Accepted: 08.12.2023

UDC 533.9.07

https://doi.org/10.31489/2024PH1/23-33

L.G. Sulyubayeva[1, 2], B.K. Rakhadilov[1], Y. Naimankumaruly[1], M.B. Bayandinova[1], N. Muktanova[1], N.E. Berdimuratov[2*]

[1]*PlasmaScience LLP, Ust-Kamenogorsk, 070000, Kazakhstan;*
[2]*Research Center Surface Engineering and Tribology, Sarsen Amanzholov East Kazakhstan University, Ust-Kamenogorsk, 070000, Kazakhstan*
[*]*Corresponding author's e-mail: nurbol.ber@gmail.com)*

Study of changes in the surface structure of tungsten irradiated by helium plasma

One of the important aspects is the interaction of plasma with the surface of a material, especially in the conditions of a fusion facility. The current work presents the preliminary results of the study of tungsten surface structure modification under helium plasma irradiation. A small-sized linear simulator KAZ-PSI with a plasma-beam setup was designed and assembled, where helium was used as a working gas. The main elements of the linear plasma simulator are an electron beam gun with a LaB6 cathode, a plasma-beam discharge chamber, an interaction chamber, a target device, and an electromagnetic system consisting of electromagnetic coils. It was revealed that under irradiation on the surface of the samples there is a relief with defective structure consisting of chaotically arranged ledges and pits of various shapes with average size (100–600) nm and pore sizes (0.1–1.5) μm with visible areas of flaking and sputtering. It was found that when the negative potential on the target is varied by –500V/–1000V/–1500V, the formation of dislocation with chaotic and cellular structure of tungsten with an average grain size of (1–25) μm is observed; it was revealed that the total values of elastic and plastic components of deformation across the tungsten grain differ from each other by about 2.5 times.

Keywords: tungsten, helium plasma, structure, surface modification, quantitative parameters of fine structure, plasma generator, surface.

Introduction

As it is known, to the present day, the successful implementation of the International Thermonuclear Experimental Reactor (ITER) project and new advances in next-generation nuclear fusion reactors such as ITER and China Fusion Engineering Test Reactor (CFETR), Demonstration Fusion Power Plant (DEMO) contribute to the development of nuclear energy and fusion and bring them to a new frontier [1–3]. Materials in fusion devices withstand severe exposure to high-temperature plasma, which promotes the development of radiation defects and subsequently leads to material damage. Therefore, the problem of improving the properties and performance characteristics of materials remains one of the important tasks for fusion energy [4]. According to the authors of the review paper [5] in the ITER facility [1], protective materials must withstand three conditions simultaneously: first, the effects of surface sputtering, blistering, and erosion during the interaction of the particles flying out of the plasma without excessive contamination of the core plasma; second, due to the rapid release of energy during plasma rupture, a relatively high steady-state surface heat load of ~10 $MW \cdot m^{-2}$ and a transient heat load of ~20 $MW \cdot m^{-2}$ are released; third, resistance to damage from neutron radiation with energy 14.1 MeV, embrittlement from hydrogen (H) isotope (deuterium (D) and tritium (T))/helium (He) and gas swelling.

Along with other energy sources, nuclear fusion is seen as the most promising alternative to fossil fuels for a future carbon-free energy system. ITER, currently the largest fusion device under construction, is expected to provide a high thermal output of ~150 MW [6]. However, the extreme conditions created during ITER operation pose significant challenges for the plasma facing materials (PFM) in the divertor of the fusion device; e.g., high heat flux deposition and particle bombardment. In the background of nuclear fusion reactor devices such as ITER and DEMO, tungsten (W) is considered as a potential and one of the most promising candidate PFM materials for plasma facing components (PFC) due to its high melting point, good thermal conductivity, low sputtering yield and low hydrogen solubility [7–8].

Helium atoms, which have low solubility in metals, can lead to undesirable changes in material properties, such as the formation of nanopores and bubbles [9, 12–13], blisters, etc. Experiments to determine the influence of helium performed in reactor experiments are very challenging due to the requirement for pro-

longed material irradiation. However, for a quick assessment of the influence of helium (hydrogen, deuterium) on material properties, valuable information is provided by simulation experiments on plasma generator stands, where atoms of the plasma-forming gas are introduced into the material through bombardment by helium ions in accelerators. In recent years, a series of experiments have been conducted on such linear simulation setups (NAGDIS-II, JULE-PSI, PISCES-A, LENTA, etc.), which have allowed important conclusions to be drawn about the nature of defects and the embrittlement and erosion mechanisms.

In the divertor, the tungsten material will face not only extreme heat fluxes but also high fluxes of low-energy particles such as deuterium, tritium, and helium. In many studies, it has been observed that exposure to helium plasma can induce the formation of nanobubbles under the tungsten surface [10, 11]. Their formation is due to the diffusion and clustering of helium atoms in the tungsten matrix [12], and the subsequent size of the nanobubbles increases as the temperature of tungsten increases during exposure [13, 14]. He atoms diffuse so rapidly and are deposited into He bubbles, causing embrittlement and curing problems in W. The rapid accumulation of He atoms also leads to microstructure evolution such as nucleation of He bubbles and subsequent formation of nano- and microscale "fluff" on the W surface at elevated temperatures, which significantly reduces the W properties themselves and affects the stability of the core plasma [15]. In the bulk of plasma facing components, He atoms can be formed by tritium decay and as a product of nuclear reactions induced by neutron irradiation. Due to the high defect binding energy, a high concentration of He can be rapidly achieved in the subsurface of PFC. This can sharply change the surface morphology and affect the erosion rate and the transfer of hydrogen isotopes into the bulk of PFC [16, 17].

Simulation facilities are very effective tools for testing candidate fusion reactor materials, to fill up the database on various aspects of plasma-surface interaction. Interest in modeling the interaction of plasma with fusion reactor material on simulation benches with gas-discharge plasma generators arose in the early eighties of the last century. With the help of ion-beam facilities, basic understanding of the elementary processes occurring under the action of ions on the surface of a solid body, such as sputtering of the material, capture and reflection of particles from it, has already been obtained. When the full-scale tokamak-reactor ITER is launched, where all damaging factors will be fully combined, one should expect the manifestation of new synergetic phenomena and effects, the study of which can rely to a large extent on the database and physical models developed in simulation experiments. At present, the Kazakhstan Materials Testing Tokamak with materials is used to test parameter measurement techniques in plasma interaction studies, and a plasma-beam facility was developed at the National Nuclear Center of the Republic of Kazakhstan in cooperation with foreign scientists to test Tokamak KTM diagnostic equipment. This plasma beam installation PBI-1 is located in the laboratory "Testing of materials under fusion reactor conditions". With the use of this unit earlier authors [18–20] carried out works on the study of plasma interaction with stainless steel, tantalum, beryllium, tungsten and molybdenum samples, where systematized results of the effect of hydrogen and deuterium plasma on the microstructure, morphology and erosion of the surface of tungsten and molybdenum were obtained [21, 22]. The results showed that the degree of surface erosion increases with increasing target temperature and ion energy. It was found that during irradiation of tungsten and molybdenum with hydrogen plasma the main relief-forming mechanism is surface sputtering and erosion is characterized by thermal etching of the surface. After irradiation with hydrogen plasma, small cracks are observed on the samples, and the size and number of cracks increase with increasing temperature. It is revealed that after irradiation the structure of tungsten is more fragmented and characterized by a more developed defect substructure. The reason for the appearance of these structural disorders seems to be mechanical stresses in the tungsten lattice caused by implanted ions. Based on the obtained results, an in-depth study of the fine structure of plasma-irradiated tungsten is proposed, and the relationship between dislocation structure and erosion processes in tungsten is also established. In this regard, the aim of the present work is to investigate the changes in the fine structure of the surface of tungsten irradiated with low-temperature helium plasma on a newly developed small-size linear divertor plasma simulator.

Materials and methods

To test materials for plasma impact, a small-size linear plasma simulator KAZ-PSI was developed and assembled in PlasmaScience LLP (Republic of Kazakhstan, Ust-Kamenogorsk), which allows simulating the operation of thermonuclear facilities, in particular Tokamak KTM. The developed linear plasma simulator KAZ-PSI is universal and allows testing of materials under conditions of complex influence on them both plasma flow and powerful thermal load created with the help of electron beam.

The main elements of the plasma unit are an electron beam gun (EBG), a plasma-beam discharge chamber, a vacuum interaction chamber, a cooling target device, and an electromagnetic system consisting of electromagnetic coils [8]. The electron beam gun consists of a heated thermoemissive cylindrical cathode made of LaB_6 and a holed anode. The cathode is heated by resistive method and a 50 kW DC power supply is used for heating. The electron beam gun is cooling by compressed air flow.

The operating principle of the KAZ-PSI plasma SLS unit is as follows: the electron gun forms an electron beam of axially symmetric character, the gun cathode is heated by electron bombardment from the heater filament, which helps to adjust the gun power. The vacuum drop between the gun and the discharge chamber is realized by autonomous pumping of the gun. The plasma cord is formed in the discharge chamber by the interaction of the electron beam with the working gas (helium). In the discharge chamber, the electromagnetic system (a system of coils), which creates a longitudinal magnetic field, focuses the electron and plasma beams. By changing the value of electric current flowing through the electromagnetic coils, it is possible to manipulate the value of magnetic field strength in the plasma beam discharge chamber, thus controlling the beam diameter. The plasma discharge hits a sample of the material under test, which is placed on a target device in the interaction chamber. General view (Fig. 1a) and schematic (1b) images of the setup are shown in Figure 1 *a–b*, where the main components of the small-size linear simulator (SLS) are indicated: electron gun, vacuum sensor, electromagnetic coils, Langmuir probe, interaction chamber, target cooling, negative potential, residual gas analyzer, turbomolecular pump, forevacuum pump, personal computer for controlling the KAZ-PSI plasma SLS.

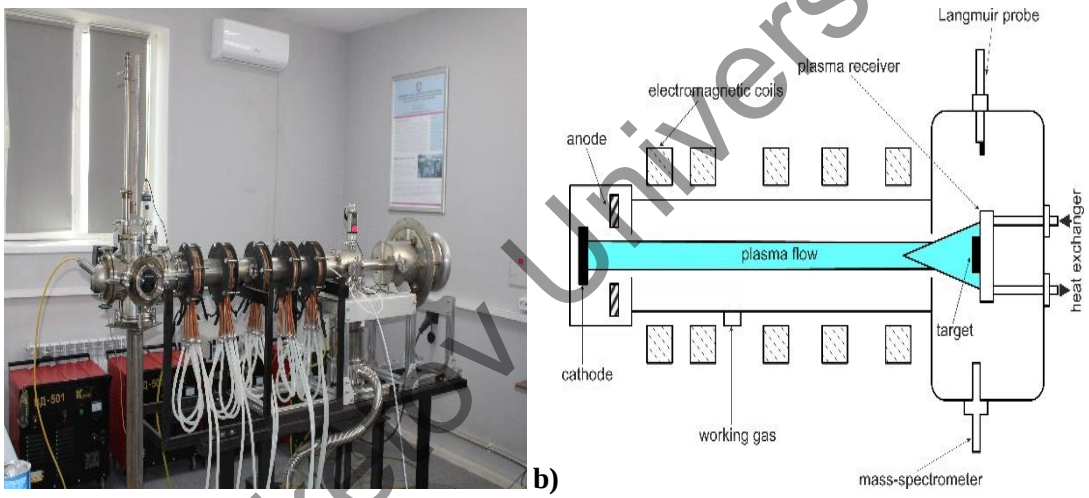

Figure 1. General view and schematic representation of KAZ-PSI plasma SLS and its main parts

Experiments in the KAZ-PSI plasma SLS were carried out in plasma-beam discharge regimes according to the previously worked out technological regimes. The samples were irradiated with helium plasma with ion energy of 1.5–2.5 keV for 3 hours, with the primary beam power of 250 W, the average value of total ion current at the target was 200–300 mA and the total ion current saturation had a value in the range of 4–8 mA. The regimes were varied according to the negative potential on the target: Regime 1 –500 V, Regime 2 –1000 V and Regime 3 –1500 V. During irradiation, the pressure in the chamber was $\sim 1.8\times10^{-3}$ Torr. Helium of special purity was used as the working gas.

In the present work, tungsten of 99.95 % purity was chosen as the research materials. Blanks of samples for research in the form of a cylinder with a diameter of 6.3 mm were made from tungsten rods. Cutting of samples was performed on a cooled cutting machine model DTQ-5 using a diamond disk with a thickness of 0.3 mm. The specimen is not subjected to thermal stress. After cutting, the specimen cuts were ground to a depth of 0.5 mm. The specimens were polished before irradiation.

Optical metallography was used to study the structure of the materials under study [7]. For metallographic analysis we used an optical light microscope “ALTAMI-MET-1M” of the Research Center “Surface Engineering and Tribology” of Sarsen Amanzholov East-Kazakhstan University and PlasmaScience LLP. The samples for research were prepared according to the standard technique, including mechanical grinding and mechanical polishing. Polishing was carried out on a grinding disk covered with felt, pre-washed and soaked in water for 1–2 hr. Chemical etching in a solution containing 50 % hydrofluoric acid and 50 % nitric

acid was used to reveal the microstructure of tungsten. To study the fine structure of the surface layer, a Philips CM30 transmission electron microscope at an accelerating voltage of 125–300 kV with an energy-dispersive micro (nano) analysis system was used [10]. The studies were carried out by diffraction electron microscopy of thin foils at an accelerating voltage of 125 kV. The working magnification in the microscope column was chosen from 10000 to 80000 magnification. Roughness was measured using the Confocal 3D profilometer Leica DCM8 SR.

Results and discussion

Figure 2 shows the microstructure of the tungsten surface before (Fig. 2*a*) and after helium plasma irradiation (Fig. 2*b*) at a potential difference of –1000 V. It is possible to observe the surface change as a relief development with defective structure as a result of inhomogeneous helium saturation of the surface. The resulting relief consists of chaotically arranged ledges and pits of various shapes with an average size of (100–600) nm, and pores (0.1–1.5) μm with visible areas of flaking and sputtering, which is most likely associated with different erosion coefficients.

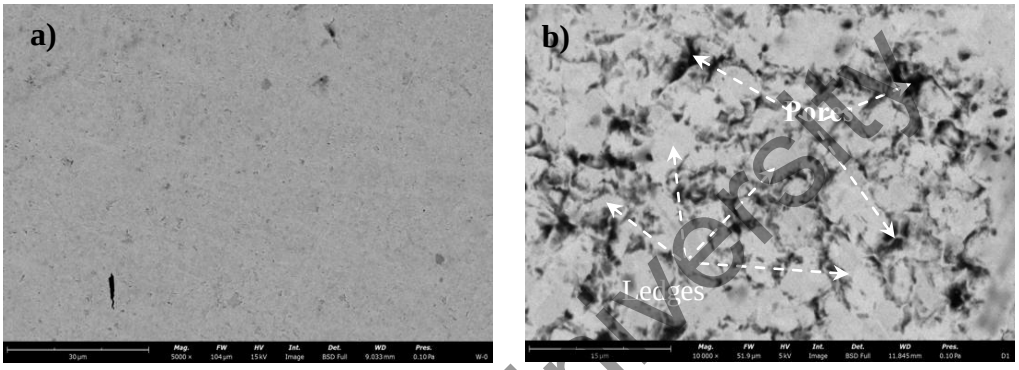

Figure 2. Tungsten surface microstructure before and after irradiation

The surface roughness of tungsten samples before and after helium plasma irradiation was evaluated using a precision tester with a diamond probe. Figure 3 *a–b* presents the forms and profiles of surface roughness along with the distribution graph of the mean arithmetic deviation of the profile across the tungsten surface before and after (–1000V) helium plasma irradiation. From Figure 3*b*, it is shown that the roughness of the surface increases by approximately 2 times after irradiation. The increase in roughness is attributed to the sputtering of the surface by helium ions, as well as the formation of blisters. According to microstructural analysis of the tungsten surface after helium plasma irradiation, defects in the form of etching pits are observed, which are confirmed by the results of roughness assessment and the conclusions of the authors [23, 24]. It is worth noting that in this process, the primary role in changing the relief is played by the sputtering of the surface by helium ions, achieved by transferring kinetic energy to the surface W atom through a cascade of successive collisions between W atoms.

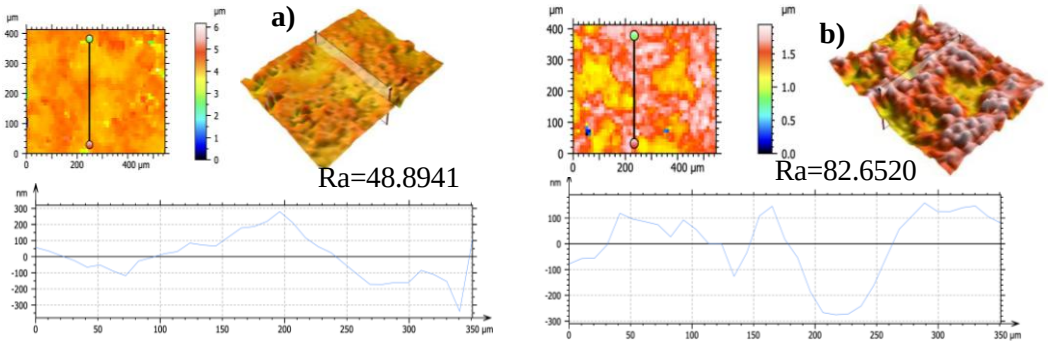

Figure 3. Tungsten surface roughness results before (*a*) and after (*b*) helium plasma irradiation

On the transmission electron microscope the fine structure of the surface (10–20 μm) of tungsten after irradiation with helium plasma was analyzed. Thus, Figure 4 shows the electron image of the fine structure

of tungsten, before and after irradiation with helium plasma. It is evident from the figure that under helium plasma irradiation a developed relief with dislocation structure is observed as a result of inhomogeneous etching of the surface, which is markedly different from the structure of the initial state of tungsten (Fig. 4*a*). The morphological component of the structure of samples after helium modification as in the initial state is tungsten, but after irradiation tungsten have defective structure (Fig. 4*b*).

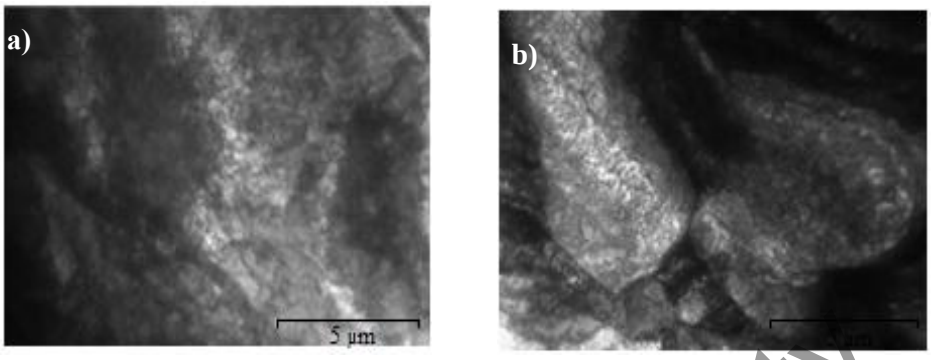

Figure 4. Electron microscopic images of the fine structure of the tungsten surface before (*a*) and after helium plasma irradiation (*b*)

When varying the negative potential on the target at –500V/–1000V/–1500V, the formation of dislocation with chaotic (Fig. 5 *b*) and cellular structure (Fig. 5 *a*, *c*) of tungsten with average grain size (1–25) μm is observed. Figure 5 shows micrographs of fine structure of tungsten surface samples irradiated by helium plasma at different target potentials (*a*) –500 V, (*b*) –1000 V, (*c*) –1500 V. According to the analysis of microphotographs of irradiated samples, it is established that in tungsten material there are intrinsic stress fields (σ) due to deformation of grains, which are localized on the grain body (Fig. 5 *d*), grain boundaries and joints (Fig. 5 *e*), ledges on intergrain boundaries (Fig. 5 *f*).

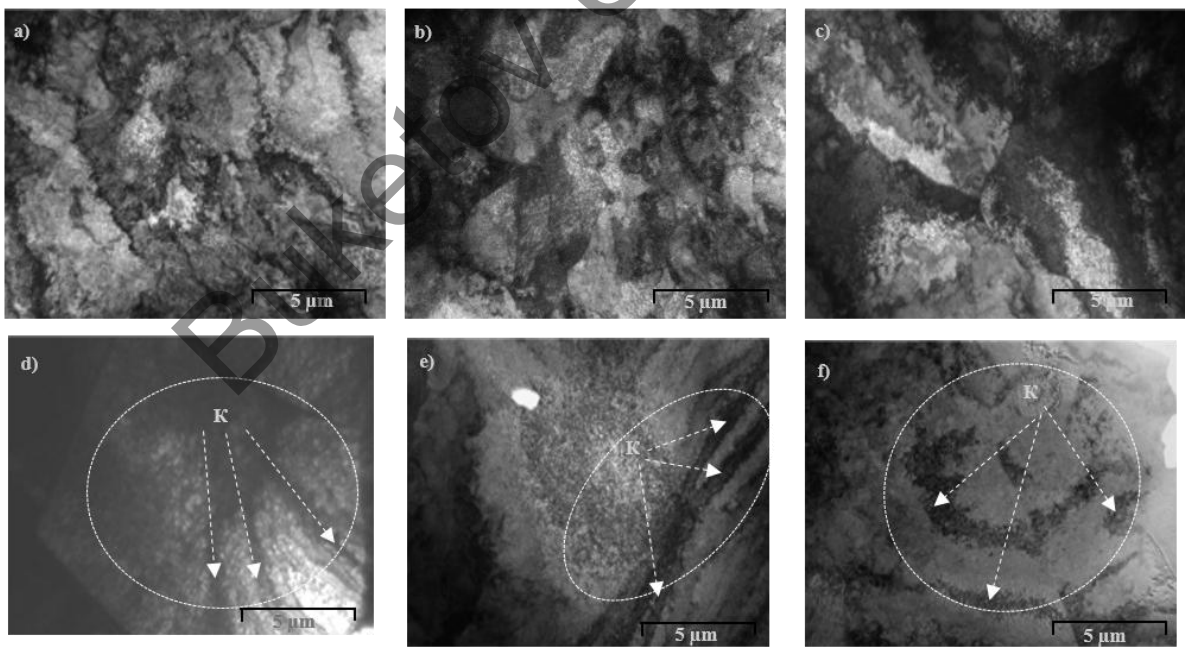

Figure 5. Micrographs of fine structure of tungsten samples irradiated by helium plasma at different target potentials

Also on electron-microscopic images Fig. 5 *d–f* it is possible to see how the internal stress fields lead to the appearance of bending extrinsic contours (denoted by the letter K) by which it is possible to determine the nature of deformation of local areas of the tungsten sample. From the available theoretical literature, it is known that the deformation is distinguished locally into elastic and plastic, mixed, as well as three types of deformation of the crystal lattice — bending, torsion and mixed type (χ). According to the method described

in [25–27], the extinction contours can be determined by the mutual orientation of the vector of the acting reflection and the extinction line, and the value of internal stresses by the elastic and plastic components of deformation. The tensor quantities were applied to the calculation as follows.

The internal bending-torsion stresses of the crystal lattice are determined as follows:

$$\sigma = \sigma_{11\text{-plas}} + \sigma_{12\text{-elas}},$$
$$\sigma_{11} = \sigma_{11\text{-plas}} + \sigma_{11\text{-elas}}, \quad (1)$$
$$\sigma_{12} = \sigma_{12\text{-plas}} + \sigma_{12\text{-elas}},$$

where $\sigma_{11\text{-plas}}$, $\sigma_{11\text{-elas}}$ and $\sigma_{12\text{-plas}}$, $\sigma_{12\text{-elas}}$ are tensors of internal bending and torsion stresses respectively [27].

Plastic and elastic components of internal stress amplitude in bending and torsion:

$$\sigma_{11\text{-plas}} = \mu\,(b\,\chi_{11\text{-plas}})^{1/2},\ \sigma_{11\text{-elas}} = \mu\,t\,\chi_{11\text{-elas}};$$
$$\sigma_{12\text{-plas}} = \mu\,(b\,\chi_{12\text{-,plas}})^{1/2},\ \sigma_{12\text{-elas}} = \mu\,t\,\chi_{12\text{-elas}}, \quad (2)$$

where μ is the elasticity modulus, b is the Burgers vector, t is the foil thickness, χ_{11} and χ_{12} are the components of the curvature-torsion amplitude tensor of the crystal lattice [27].

Thus, according to calculations, the values of stress σ belong in the range of 0–850 MPa and 1100–1980 MPa and they are localized over a larger area inside the tungsten grain. Thus, the average value of internal stress across the grain was calculated and was equal to 1560 MPa, with the tungsten strength limit of 500–1400 MPa according to the reference book. Also the components of the tensor of internal stresses of the elastic component of deformation were calculated, they are on average on the grain are equal to: bending stress σ_{11} = 620 MPa and torsion σ_{12} = 1470 MPa of the crystal lattice; the average values of the components of the tensor of internal stresses of the plastic component of deformation on the grain are equal to: bending stress σ_{11} = 350 MPa and torsion σ_{12} = 480 MPa of the crystal lattice. The total values of the components of elastic and plastic strains across the grain differ from each other by approximately 2.5 times.

Figure 6 shows electron microscopic images of the fine structure of tungsten in the initial state (*a* — light-field image, *b* — microdiffraction pattern, *c* — its indexed scheme) and after irradiation (*d* — light-field image, *e* — microdiffraction pattern, *f* — indexed scheme) where there are embedding reflections in the form of carbide. According to microdiffraction studies, grain boundary etching is observed, the internal structure of tungsten and carbide grains are clearly expressed. Grain boundaries are clearly revealed, inside the grains there is already well enough expressed modified substructure and defective microstructure.

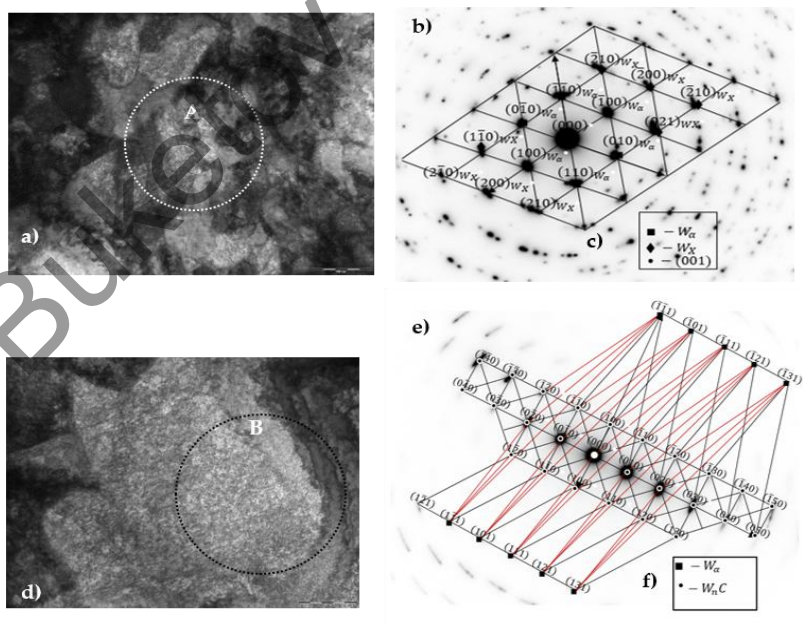

Figure 6. Electron microscopic images of the fine structure of tungsten and their microdiffraction patterns

Thus, modification of tungsten with helium leads to defectively that apparently approaches the defectively of matrix grain boundaries. The possibility of formation of such substructure of grains at helium plasma irradiation is provided by the increased energy state of the surface and subsurface layers exposed throughout the irradiation and neutral atoms of low-temperature plasma. Tungsten carbide particles, which were apparently a residual product inside the chamber, can be located in different morphological components

of the matrix. In fact, carbide can localize at matrix grain boundaries and in the grain body, as in (Fig. 5 *d*). According to the studies, carbide was not bound to the boundaries but is a product of matrix delamination in α-WC or β-WC. These localizations are mostly related to crystal structure defects [28].

Conclusions

Thus, summarizing the above results we can draw the following main conclusions of this paper:

– the simulation stand of the small-size linear plasma simulator KAZ-PSI with a plasma-beam unit opens the possibility to test and justify the choice of candidate fusion reactor materials under different operating conditions, as well as significantly expands the available results on various aspects of plasma-surface interaction and helps to reliably harmonize computational models and work out diagnostic methodologies under sufficiently well-programmed conditions;

– conducted preliminary experiments to investigate changes in the structure of tungsten under helium plasma irradiation, showed that after irradiation on the surface is formed relief with defective structure, consisting of chaotically located ledges and pits of various shapes with an average size of (100–600) nm, and pores with sizes (0.1–1.5) μm with visible areas of flaking and sputtering;

– it is found that by varying the negative potential on the target by –500 V/–1000 V/–1500 V, the formation of dislocation with chaotic and cellular structure of tungsten with an average grain size of (1–25) μm was observed;

– determined that the values of internal stress σ lie in the range 0–850 MPa and 1100–1980 MPa;

– it is revealed that the total values of elastic and plastic components of deformations across the tungsten grain differ from each other approximately 2.5 times;

– it is found that modification of tungsten with helium leads to defectively, which is apparently close to the defectively of the grain boundaries of the matrix, not leading to the destruction of the material.

Acknowledgments

This research is funded by the Science Committee of the Ministry of Science and Higher Education of the Republic of Kazakhstan (Grant No.BR21882370).

References

1 Neilson G.H Summary of the international workshop on magnetic fusion energy (MFE) roadmapping in the ITER era / G.H. Neilson, G. Federici, J. Li, D. Maisonnier, R. Wolf // Nuclear Fusion. — 2012. — 52(4). — 047001. https://doi.org/10.1088/0029-5515/52/4/047001.

2 Wan Y. Overview of the present progress and activities on the CFETR / Y. Wan, J. Li, Y. Liu, X. Wang, V. Chan, C. Chen, X. Duan, P. Fu, X. Gao, K. Feng, S. Liu, Y. Song, P. Weng, B. Wan, F. Wan, H. Wang, S. Wu, M. Ye, Q. Yang, G. Zheng, G. Zhuang, Q. Li // Nuclear Fusion. — 2017. — 57(10). — 102009. https://doi.org/10.1088/1741-4326/aa686a.

3 Zohm H. On the physics guidelines for a tokamak DEMO / H. Zohm, C. Angioni, E. Fable, G. Federici, G. Gantenbein, T. Hartmann, K. Lackner, E. Poli, L. Porte, O. Sauter, G. Tardini, D. Ward, M. Wischmeier // Nuclear Fusion. — 2013. — 53(7). — 073019. https://doi.org/10.1088/0029-5515/53/7/073019.

4 Zinkle S.J. Fusion materials science and technology research opportunities now and during the ITER era / S.J. Zinkle, J.P. Blanchard, R.W. Callis, C.E. Kessel, R.J. Kurtz, P.J. Lee, K.A. McCarthy, N.B. Morley, F. Najmabadi, R.E. Nygren, G.R. Tynan, D.G. Whyte, R.S. Willms, B.D. Wirth // Fusion Engineering and Design. — 2014. — 89(7–8). — 1579. https://doi.org/10.1016/j.fusengdes.2014.02.048.

5 Li Y.G. A review of surface damage/microstructures and their effects on hydrogen/helium retention in tungsten / Y.G. Li, Q.R. Zheng, L.M. Wei, C.G. Zhang, Z. Zeng // Tungsten. — 2020. — 2. — P. 34–71. https://doi.org/10.1007/s42864-020-00042-w.

6 Kallenbach A. The ASDEX Upgrade Team. Impurity seeding for tokamak power exhaust: from present devices via ITER to DEMO / A. Kallenbach, M. Bernert, R. Dux, L. Casali, T. Eich, L. Giannone, A. Herrmann, R. McDermott, A. Mlynek, H. Müller, F. Reimold, J. Schweinzer, M. Sertoli, G. Tardini, W. Treutterer, E. Viezzer, R. Wenninger, M. Wischmeier // Plasma Physics and Controlled Fusion. — 2013. — 55(12). — 124041. https://doi.org/10.1088/0741-3335/55/12/124041.

7 Салтыков С.А. Стереометрическая металлография / С.А. Салтыков. — М.: Металлургия, 1976. — С. 190.

8 Pitts R.A. Physics basis for the first ITER tungsten divertor / R.A. Pitts, X. Bonnin, F. Escourbiac, H. Frerichs, J.P. Gunn, T. Hirai, A.S. Kukuushkin, E. Kakeeva, M.A. Miller, D. Moulton, V. Rozhansky, I. Senichenkov, E. Sytova, O. Schmitz // Nuclear Materials and Energy. — 2019. — P. 20. — 100696. https://doi.org/10.1016/j.nme.2019.100696.

9 Balooch M. Mechanical and structural transformations of tungsten implanted with helium ions / M. Balooch, F.I. Allen, M.P. Popovic, P. Hosemann // Journal of Nuclear Materials. — 2022. — Vol. 559. — 153436. https://doi.org/10.1016/j.jnucmat.2021.153436.

10 Эндрюс К. Электронограммы и их интерпретация / К. Эндрюс, Д. Дайсон, С. Киоун. — М.: Мир, 1971. — 256 с.

11 Perez D. Diffusion and transformation kinetics of small helium clusters in bulk tungsten / D. Perez, T. Vogel, B.P. Uberuaga // *Phys. Rev. B.* – 2014. — 90. — 14102. https://doi.org/10.1103/PhysRevB.90.014102.

12 Miyamoto M. Systematic investigation of the formation behavior of helium bubbles in tungsten / M. Miyamoto, S. Mikami, H. Nagashima, N. Iijima, D. Nishijima, R. Doerner, N. Yoshida, H. Watanabe, Y. Ueda, A. Sagara // Nuclear Materials. — 2015. — P. 463. — 333–6. https://doi.org/10.1016/j.jnucmat.2014.10.098.

13 Thompson M. Measuring temperature effects on nano-bubble growth in tungsten with grazing incidence small angle x-ray scattering / M. Thompson, R. Doerner, N. Ohno, N. Kirby, P. Kluth, D. Riley, C. Corr // Nuclear Materials and Energy. — 2017. — P. 121294–1297. https://doi.org/10.1016/j.nme.2016.11.025.

14 Qin W. Nanochannel structures in W enhance radiation tolerance / W. Qin, F. Ren, R.P. Doerner, G. Wei, Y. Lv, S. Chang, M. Tang, H. Deng, C. Jiang, Y. Wang // ActaMaterialia. — 2018. — 153. — P. 147–155. https://doi.org/10.1016/j.actamat.2018.04.048.

15 Tulenbergenov T. Interaction between nitrogen plasma and tungsten / T. Tulenbergenov, M. Skakov, A. Kolodeshnikov, V. Zuev, B.K. Rakhadilov, I. Sokolov, D. Ganovichev, A. Miniyazov, O. Bukina // Nuclear Materials and Energy. — 2017. — 13. — P. 63–67. https://doi.org/10.1016/j.nme.2017.07.005.

16 Tulenbergenov T.R. Formation of “Fuzz” on the Pre-Nitrided Tungsten Surface / T.R. Tulenbergenov, M.K. Skakov, I.A. Sokolov, D.A. Ganovichev // Physics of Atomic Nuclei. — 2019. — 82(11). — 1454–1459. https://doi.org/10.1134/S1063778819120299.

17 Sokolov I.A. Study of the Interaction of Plasma with Berylli um That Is a Candidate Material for the First Wall of a Fusion Reactor / I.A. Sokolov, M.K. Skakov, V.A. Zuev, D.A. Ganovichev, T.R. Tulenbergenov, A.Z. Miniyazov // Technical Physics. — 2018. — P. 63. — 506–510. https://doi.org/10.1134/S1063784218040230.

18 Tulenbergenov T.R. Studies on gas release from pre-saturated samples on a plasma beam installation / T.R. Tulenbergenov, T.V. Kulsartov, I.A. Sokolov, B.K. Rakhadilov, D.A. Ganovichev, A.J. Miniyazov, A.A. Sitnikov // Physical Sciences and Technology. — 2017. — 4(2). — P. 15–28. https://doi.org/10.26577/phst-2017-2-130.

19 Rakhadilov B.K. Tungsten Surface Erosion by Hydrogen Plasma Irradiation / B.K. Rakhadilov, M.K. Skakov, T.R. Tulenbergenov // Key Engineering Materials. — 2017. — 736, 46–51. https://doi.org/10.4028/www.scientific.net/KEM.736.46.

20 Рахадилов Б.К. Патент РК № 22: Установка для моделирования взаимодействия плазмы с кандидатными материалами термоядерного реактора / Б.К. Рахадилов, М.К. Скаков, Т.Р. Туленбергенов. — 2017. — Бюл. — № 2.

21 Rakhadilov B.K. Plasma installation for research of plasma-surface interaction / B.K. Rakhadilov, M. Skakov, T. Tulenbergenov, L. Zhurerova, Sh. Kurbanbekov // Eurasian Physical Technical Journal. — 2019. — 16. — P. 36–42. https://doi.org/10.31489/2019No2/36-42.

22 Rakhadilov B. Hydrogen and deuterium storage in tungsten when irradiation with plasma beam / B. Rakhadilov, M. Skakov, A. Miniyzov, A. Kengesbekov // Conference Proceedings. — 2018. — P. 1216–1221.

23 Xuechun Li In-situ measurements of low energy D plasma-driven permeation through He pre-damaged W / Li Xuechun, Zhoua Hai-Shan, Liua Hao-Dong, Wanga Lu, Luo Guang-Nan // Nuclear Fusion. — 2021. — P. 1–15. https://doi.org/10.1088/1741-4326/ac4716.

24 You Sung Phase-Field Study of Microstructure Evolution in Tungsten Polycrystalline under He/D Irradiation / Sung You, A. Han // Materials. — 2021. — 14(23). — 7433. https://doi.org/10.3390/ma14237433.

25 Уманский Я.С. Физическое металловедение / Я.С. Уманский, Б.Н. Финкельштейн, М.Е. Блантер и др. — М.: Гос. науч.-тех. изд-во литературы по чёрной и цветной металлургии, 1955. — С. 721.

26 Koneva N.A. Determination of the energy density stored during plastic deformation of an isotropic body, according to curvature-torsion of the crystal lattice / N.A. Koneva, S.F. Kiseleva, N.A. Popova, E.V. Kozlov // Fundamental Problems and Modern Technologies of Material Science. — 2011. — 3. — 34.

27 Киселева С.Ф. Распределение внутренних напряжений и плотности запасенной энергии внутри отдельного зерна деформированного поликристалла / С.Ф. Киселева, Н.А. Попова, Н.А. Конева, Э.В. Козлов // Письма о материалах. — 2012. — Т. 2. — С. 84–89. https://doi.org/10.22226/2410-3535-2012-2-84-89.

28 Рахадилов Б.К. Изменение поверхности вольфрама при облучении плазменным пучком / Б.К. Рахадилов, М.К. Скаков, Т.Р. Туленбергенов, В.К. Виелеба // Вестн. Караганд. ун-та. Сер. Физика. — 2016. — № 3(83).

Л.Г. Сулюбаева, Б.К. Рахадилов, Е. Найманқұмаруұлы,
М.Б. Баяндинова, Н. Мұқтанова, Н.Е. Бердимуратов

Төментемпературалы гелий плазмасымен сәулеленген вольфрам бетінің құрылымының өзгеруін зерттеу

Термоядролық қондырғы жағдайындағы ең маңызды аспектілердің бірі плазманың материалдың бетімен әрекеттесуі. Мақалада гелий плазмасымен сәулелену кезіндегі вольфрам бетінің құрылымын өзгертуді зерттеудің алдын-ала нәтижелері келтірілген. Гелий жұмыс газы ретінде пайдаланылған плазмалық-сәулелік қондырғысы бар шағын көлемді сызықтық Каз-ПСИ симуляторы әзірленді және құрастырылды. Сызықтық плазмалық имитатордың негізгі элементтері LaB_6 катодты электронды

сәулелік зеңбірек, плазмалық сәулелік разряд камерасы, өзара әрекеттесу камерасы, нысаналық құрылғы және электромагниттік катушкалардан тұратын электромагниттік жүйе. Сәулелену кезінде үлгілердің бетінде орташа мөлшері (100–600) нм және кеуек өлшемдері (0,1–1,5) мкм, қабыршықтану мен тозаңданудың көрінетін жерлері бар, әр түрлі пішіндегі ретсіз орналасқан дөңестер мен шұңқырлардан тұратын ақаулы құрылымы бар рельеф пайда болатыны анықталды. Нысанаға теріс потенциал -500В/-1000В/-1500В өзгерген кезде орташа түйіршік мөлшері (1–25) мкм болатын ретсіз және ұяшықты вольфрам құрылымы бар дислокациялардың пайда болуы байқалады; вольфрам түйіршігі бойынша деформацияның серпімді және пластикалық компоненттерінің жиынтық мәндері бір-бірінен шамамен 2,5 есе ерекшеленетіні анықталды.

Кілт сөздер: вольфрам, гелий плазмасы, құрылымы, беттің модификациясы, жұқа құрылымның сандық параметрлері, плазмалық генератор, беті.

Л.Г. Сулюбаева, Б.К. Рахадилов, Е. Найманқұмаруұлы,
М.Б. Баяндинова, Н. Мұқтанова, Н.Е. Бердімуратов

Исследование изменения структуры поверхности вольфрама, облученного низкотемпературной гелиевой плазмой

Одним из важных аспектов является взаимодействие плазмы с поверхностью материала, особенно в условиях термоядерной установки. В статье представлены предварительные результаты исследования модификации структуры поверхности вольфрама при облучении гелиевой плазмой. Был разработан и смонтирован малогабаритный линейный симулятор КАЗ-ПСИ с плазменно-пучковой установкой, где в качестве рабочего газа использовался гелий. Основными элементами линейного плазменного имитатора являются электронно-пучковая пушка с катодом из LaB6, камера плазменно-пучкового разряда, камера взаимодействия, мишенное устройство и электромагнитная система, состоящая из электромагнитных катушек. Обнаружено, что при облучении на поверхности образцов образуется рельеф с дефектной структурой, состоящей из хаотично расположенных выступов и ямок различной формы со средним размером (100–600) нм и размерами пор (0,1–1,5) мкм с видимыми участками шелушения и напыления. Установлено, что при изменении отрицательного потенциала на мишени на –500 В/–1000 В/–1500 В наблюдается образование дислокаций с хаотической и ячеистой структурой вольфрама со средним размером зерна (1–25) мкм; выявлено, что суммарные значения упругой и пластической составляющих деформации по зерну вольфрама отличаются друг от друга примерно в 2,5 раза.

Ключевые слова: вольфрам, гелиевая плазма, структура, модификация поверхности, количественные параметры тонкой структуры, плазменный генератор, поверхность.

References

1 Neilson, G.H., Federici, G., Li, J., Maisonnier, D., & Wolf, R. (2012). Summary of the international workshop on magnetic fusion energy (MFE) roadmapping in the ITER era. *Nuclear Fusion, 52*(4), 047001. https://doi.org/10.1088/0029-5515/52/4/047001.

2 Wan, Y., Li, J., Liu, Y., Wang, X., Chan, V., Chen, C., Duan, X., Fu, P., Gao, X., Feng, K., Liu, S., Song, Y., Weng, P., Wan, B., Wan, F., Wang, H., Wu, S.,Ye, M., Yang, Q., Zheng, G., Zhuang, G., & Li, Q. (2017). Overview of the present progress and activities on the CFETR. *Nuclear Fusion, 57*(10), 102009. https://doi.org/10.1088/1741-4326/aa686a.

3 Zohm, H., Angioni, C., Fable, E., Federici, G., Gantenbein, G., Hartmann, T., Lackner, K., Poli, E., Porte, L., Sauter, O., Tardini, G., Ward, D., & Wischmeier, M. (2013). On the physics guidelines for a tokamak DEMO. *Nuclear Fusion, 53*(7), 073019. https://doi.org/10.1088/0029-5515/53/7/073019.

4 Zinkle, S.J., Blanchard, J.P., Callis, R.W., Kessel, C.E., Kurtz, R.J., Lee, P.J., McCarthy, K.A., Morley, N.B., Najmabadi, F., Nygren, R.E., Tynan, G.R., Whyte, D.G., Willms, R.S., & Wirth, B.D. (2014). Fusion materials science and technology research opportunities now and during the ITER era. *Fusion Engineering and Design, 89*(7–8), 1579. https://doi.org/10.1016/j.fusengdes.2014.02.048

5 Li, Y.G., Zheng, Q.R., Wei, L.M., Zhang, C.G., & Zeng, Z. (2020). A review of surface damage/microstructures and their effects on hydrogen/helium retention in tungsten. *Tungsten, 2*, 34–71. https://doi.org/10.1007/s42864-020-00042-w.

6 Kallenbach, A., Bernert, M., Dux, R., Casali, L., Eich, T., Giannone, L., Herrmann, A., McDermott, R., Mlynek, A., Müller, H., Reimold, F., Schweinzer, J., Sertoli, M., Tardini, G., Treutterer, W., Viezzer, E., Wenninger, R., & Wischmeier, M. (2013). The ASDEX Upgrade Team. Impurity seeding for tokamak power exhaust: from present devices via ITER to DEMO. *Plasma Physics and Controlled Fusion, 55*(12), 124041. https://doi.org/10.1088/0741-3335/55/12/124041.

7 Saltykov, S.A. (1976). *Stereometricheskaia metallografiia [Metallografia stereometrica]*. Moscow: Metallurgiia [in Russian].

8 Pitts, R.A., Bonnin, X., Escourbiac, F., Frerichs, H., Gunn, J.P., Hirai, T., Kukuushkin, A.S., Kakeeva, E., Miller, M.A., Moulton, D., Rozhansky, V., Senichenkov, I., Sytova, E., & Schmitz, O. (2019). Physics basis for the first ITER tungsten divertor. *Nuclear Materials and Energy*, 20, 100696. https://doi.org/10.1016/j.nme.2019.100696.

9 Balooch, M., Allen, F.I., Popovic, M.P., & Hosemann, P. (2022). Mechanical and structural transformations of tungsten implanted with helium ions. *Journal of Nuclear Materials, 559*, 153436. https://doi.org/10.1016/j.jnucmat.2021.153436.

10 Endryus, K., Dajson, D., & Kioun, S. (1971). Elektronogrammy i ikh interpretatsiia [Electronograms and their interpretation]. Moscow: Mir [in Russian].

11 Perez, D., Vogel, T., & Uberuaga, B.P. (2014). Diffusion and transformation kinetics of small helium clusters in bulk tungsten. *Phys. Rev. B., 90*, 14102. https://doi.org/10.1103/PhysRevB.90.014102.

12 Miyamoto, M., Mikami, S., Nagashima, H., Iijima, N., Nishijima, D., Doerner, R., Yoshida, N., Watanabe, H., Ueda, Y., & Sagara, A. (2015). Systematic investigation of the formation behavior of helium bubbles in tungsten. *Nuclear Materials*, 463, 333–6. https://doi.org/10.1016/j.jnucmat.2014.10.098.

13 Thompson, M., Doerner, R., Ohno, N., Kirby, N., Kluth, P., Riley, D., & Corr, C. (2017). Measuring temperature effects on nano-bubble growth in tungsten with grazing incidence small angle x-ray scattering. *Nuclear Materials and Energy*, 121294–1297. https://doi.org/10.1016/j.nme.2016.11.025.

14 Qin, W., Ren, F., Doerner, R.P., Wei, G., Lv, Y., Chang, S., Tang, M., Deng, H., Jiang, C., & Wang, Y. (2018). Nanochannel structures in W enhance radiation tolerance. *ActaMaterialia, 153*, 147–155. https://doi.org/10.1016/j.actamat.2018.04.048.

15 Tulenbergenov, T., Skakov, M., Kolodeshnikov, A., Zuev, V., Rakhadilov, B.K., Sokolov, I., Ganovichev, D., Miniyazov, A., & Bukina, O. (2017). Interaction between nitrogen plasma and tungsten. *Nuclear Materials and Energy*, *13*, 63-67. https://doi.org/10.1016/j.nme.2017.07.005.

16 Tulenbergenov, T.R., Skakov, M.K., Sokolov, I.A., & Ganovichev, D.A. (2019). Formation of "Fuzz" on the Pre-Nitrided Tungsten Surface. *Physics of Atomic Nuclei, 82*(11), 1454–1459. https://doi.org/10.1134/S1063778819120299.

17 Sokolov, I.A., Skakov, M.K., Zuev, V.A., Ganovichev, D.A., Tulenbergenov, T.R., & Miniyazov, A.Z. (2018). Study of the Interaction of Plasma with Beryllium That Is a Candidate Material for the First Wall of a Fusion Reactor. *Technical Physics*, *63*, 506-510. https://doi.org/10.1134/S1063784218040230.

18 Tulenbergenov, T.R., Kulsartov, T.V., Sokolov, I.A., Rakhadilov, B.K., Ganovichev, D.A., Miniyazov, A.J., & Sitnikov, A.A. (2017). Studies on gas release from pre-saturated samples on a plasma beam installation. *Physical Sciences and Technology, 4*(2), 15–28. https://doi.org/10.26577/phst-2017-2-130.

19 Rakhadilov, B.K., Skakov, M.K. & Tulenbergenov, T.R. (2017). Tungsten Surface Erosion by Hydrogen Plasma Irradiation. *Key Engineering Materials, 736*, 46–51. https://doi.org/10.4028/www.scientific.net/KEM.736.46.

20 Rahadilov, B.K., Skakov, M.K., & Tulenbergenov, T.R. (2017). Patent RK № 22: Ustanovka dlia modelirovaniia vzaimodeistviia plazmy s kandidatnymi materialami termoiadernogo reaktora [Patent of the Republic of Kazakhstan No. 22 Installation for modeling plasma interaction with candidate materials of a thermonuclear reactor]. Biulleten, 2 [in Russian].

21 Rakhadilov, B.K., Skakov, M., Tulenbergenov, T., Zhurerova, L., & Kurbanbekov, Sh. (2019). Plasma installation for research of plasma-surface interaction. *Eurasian Physical Technical Journal, 16*, 36-42. https://doi.org/10.31489/2019No2/36-42.

22 Rakhadilov, B., Skakov, M., Miniyzov, A., & Kengesbekov, A. (2018). Hydrogen and deuterium storage in tungsten when irradiation with plasma beam. *Conference Proceedings,* 1216–1221.

23 Xuechun, Li, Hai-Shan, Zhoua, Hao-Dong, Liua, Lu, Wanga, & Guang-Nan, Luo. (2021). In-situ measurements of low energy D plasma-driven permeation through He pre-damaged W. *Nuclear Fusion*, 1–15. https://doi.org/10.1088/1741-4326/ac4716

24 You, Sung & Han, A. (2021). Phase-Field Study of Microstructure Evolution in Tungsten Polycrystalline under He/D Irradiation. *Materials, 14*(23), 7433. https://doi.org/10.3390/ma14237433

25 Umanskij, Ya.S., Finkel'shtejn, B.N., & Blanter, M.E. et al. (1955). Fizicheskoe metallovedenie [Physical metallurgy]. Moscow: Gosudarstvennoe nauchno-tekhnicheskoe izdatelstvo literatury po chernoi i tsvetnoi metallurgii [in Russian].

26 Koneva, N.A., Kiseleva, S.F., Popova, N.A., & Kozlov, E.V. Determination of the energy density stored during plastic deformation of an isotropic body, according to curvature-torsion of the crystal lattice. *Fundamental Problems and Modern Technologies of Material Science, 3*, 34.

27 Kiseleva, S.F., Popova, N.A., Koneva, N.A., & Kozlov, E.V. (2012). Raspredelenie vnutrennikh napriazhenii plotnosti zapasennoi energii vnutri otdelnogo zerna deformirovannogo polikristalla [Distribution of internal stresses and stored energy density inside a single grain of deformed polycrystal]. *Pisma o materialakh — Letters about materials, 2*, 84–89. https://doi.org/10.22226/2410-3535-2012-2-84-89 [in Russian].

28 Rakhadilov, B.K., Skakov, M.K., Tulenbergenov, T.R., & Wieleba, W.K. (2016). Izmenenie poverkhnosti volframa pri obluchenii plazmennym puchkom [Change the tungsten surface when irradiated by plasma beam]. *Bulletin of the University of Karaganda-Physics, 3*(83) [in Russian].

Information about authors

Sulyubayeva, L.G. — PhD, Associate professor, Senior Researcher of Scientific Research Center "Surface Engineering and Tribology", S. Amanzholov East Kazakhstan University, Ust-Kamenogorsk, Kazakhstan; e-mail: lsulyubayeva@gmail.com, https://orcid.org/0000-0002-1924-1459

Rakhadilov, B.K. — PhD, Associate professor, Director of "PlasmaScience" LLP, Ust-Kamenogorsk, Kazakhstan; e-mail: rakhadilovb@mail.ru, ORCID iD: https://orcid.org/0000-0001-5990-7123

Naimankumaruly, Y. — PhD student of Shakarim University, Semey; Researcher of "PlasmaScience" LLP, Ust-Kamenogorsk, Kazakhstan; e-mail: naimankumarylu@gmail.com, https://orcid.org/0009-0005-1953-316X

Bayandinova, M.B. — PhD student of Sarsen Amanzholov EKU, researcher of "PlasmaScience" LLP, Ust-Kamenogorsk, Kazakhstan, e-mail: shohmanovamb@gmail.com

Muktanova, N. — PhD student of D. Serikbayev East Kazakhstan Technical University, Researcher of "PlasmaScience" LLP. E-mail: muktanovan@gmail.com, https://orcid.org/0000-0002-4823-6640

Berdimuratov, N.E. — Junior researcher of scientific research center "Surface engineering and tribology", Sarsen Amanzholov East Kazakhstan University, Ust-Kamenogorsk, Kazakhstan; e-mail: nurbol.ber@gmail.com. ORCID ID: https://orcid.org/0009-0000-6880-6439